Netherlands Journal of Sea Research
24 (2/3): 287-301 (1989)

PALAEOMAGNETISM OF CRETACEOUS SEDIMENTS FROM MISOOL, NORTHEASTERN INDONESIA

HANS WENSINK[1], SUHARNO HARTOSUKOHARDJO[2] and YAN SURYANA[2]
[1]*Palaeomagnetic Laboratory, Institute of Earth Sciences, P.O. Box 80.021, 3508 TA Utrecht, The Netherlands*
[2]*Marine Geological Institute, Jalan Dr. Junjunan 236, Bandung 40135, Indonesia*

ABSTRACT

Palaeomagnetic analysis of Mesozoic pelagic sediments of the island of Misool, northeast Indonesia, showed that a large part of the sediments have very low initial remanence intensities. Progressive demagnetization both with alternating magnetic fields and with heating yielded characteristic remanence directions in two formations: the Waaf Formation of Santonian age revealed the following data: D = 318.1°, I = −33.8°, with a_{95} = 4.9°; the Fafanlap Formation of middle Maastrichtian age gave: D = 176.1°, I = 38.3°, with a_{95} = 5.1°. The fold-test applied to the Waaf Formation was positive. Pole positions derived from the rocks of Misool do not coincide with those of Australian rocks of approximately the same age. Very probably, Misool formed part of the microcontinents that split off from Australia in late Triassic-Jurassic times. In the late Cretaceous Misool was positioned at a palaeolatitude of 20° south. At that time the crustal fragment of Misool was located at least 1000 km to the north-northwest or northwest of Misool's present position, and thus far away from Australia. Since late Cretaceous time Misool has moved northwards, but not as fast as the Australian continent. Misool has undergone an anticlockwise rotation of approximately 20° relative to Australia.

1. INTRODUCTION

The Island of Misool was visited within the framework of the Indonesian-Dutch Snellius-II Expedition (Campaign GF 3) for the purpose of collecting oriented samples for palaeomagnetic research. The Island of Misool is located southwest of Bird's Head, the westernmost extension of Irian Jaya, the Indonesian part of the Island of New Guinea (Fig. 1). Misool lies in the Seram Sea at a longitude of 130°E and a latitude of 2°S. The island is about 80 km long and 50 km wide. Misool was selected for a palaeomagnetic study, because the island exhibits a rather complete stratigraphic record from middle Triassic times onwards. The sediments of Jurassic and Cretaceous age looked promising for this palaeomagnetic investigation, because they are largely bathyal deposits.

The palaeomagnetic data derived from these Misool sediments will be compared with those obtained from Australian rocks of the same age, and the position of Misool will be considered with respect to the main Australian continent.

Acknowledgments.—This research has been carried out as a part of the Snellius-II Expedition, organized by the Netherlands Council of Oceanic Research (NRZ) and the Indonesian Institute of Science (LIPI). The authors are grateful to the staff of the Palaeomagnetic Laboratory of Utrecht State University for their interest in this study. We are much obliged to Nasrun Darwin and Dida Kusnida for assistance in the field. Drs. J.L. Kool joined the expedition; his help is greatly appreciated.

2. GEOLOGY OF MISOOL

The Island of Misool is of special geological interest, because it is the only place for hundreds of miles around with a well-exposed fairly complete stratigraphic record going back to the early Mesozoic. Misool has attracted many scientists; consequently, its geology is well known (ROGGEVEEN, 1939; VAN BEMMELEN, 1949; FROIDEVEAUX, 1974; PIGRAM *et al.*, 1982). Basement rocks are exposed on the southwestern coast of the island. These low-grade Ligu Metamorphics possibly have a late Palaeozoic age.

The metamorphics are covered, with angular unconformity, by a more than 1000 m thick sequence of rhythmically bedded sandstones and shales in flysch facies of the Triassic Keskain Formation (Fig. 2). These deep-water sediments are largely folded and faulted, and are overlain, with an angular unconformity, by shallow marine reef limestones of the Bogal Formation which is of late Triassic age.

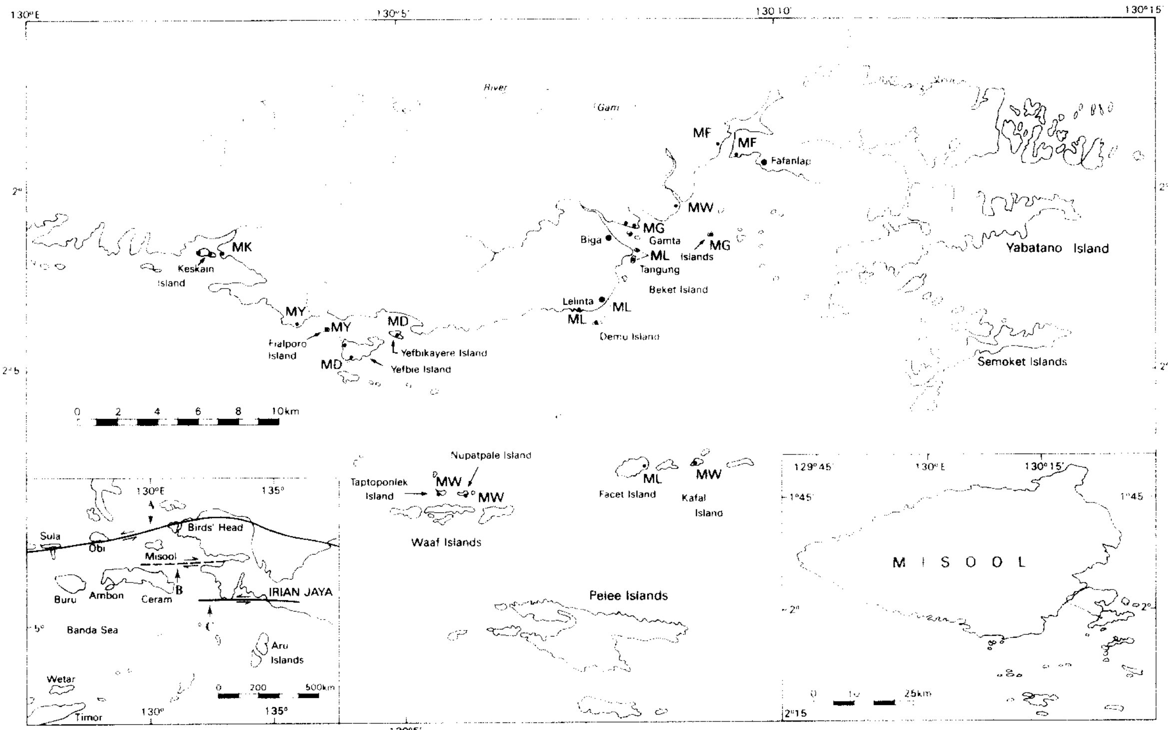

Fig. 1. Map of Misool showing the palaeomagnetic sampling localities: MK is Keskain Formation (Fm); MY is Yefbie Fm; MD is Demu Fm; ML is Lelinta Fm; MG is Gamta Fm; MW is Waaf Fm; and MF is Fafanlap Fm. Inset map below left shows some main faults: A is Sorong Fault; B is Bintuni Fault; and C is Tarera Fault.

Coarse sandstones and conglomerates of Jurassic age overlie an erosional surface. On top of these clastics follows the deposition of 80 m of grey calcareous shales and siltstones of the early Jurassic Yefbie Shale Formation pointing to restricted marine conditions. Afterwards, open marine conditions prevailed until late Cretaceous time when calcilutites were deposited with some intercalated shales or marls.

PIGRAM *et al.* (1982) distinguished two successive groups: the Fageo Group and the overlying Facet Limestone Group. The Fageo Group is composed of three formations. On top of the Yefbie Shales follows the Demu Formation with 80 m of well-bedded, grey silty limestones, marls, and shales with some bioturbation. These bathyal deposits are covered by about 100 m of grey, calcareous and non-calcareous shales and marls of the Lelinta Shale Formation which is of late Jurassic age. The Facet Limestone Group embraces the greater part of the Cretaceous time interval, and consists of two formations: the Gamta Limestone Formation and the Waaf Limestone Formation, each being about 80 m thick. The Gamta Limestone is built up of white, well-bedded calcilutites with some cherts; the overlying Waaf Limestone consists of well-bedded, partly maroon, tuffaceous calcilutites. On top of these bathyal deposits follow conformably about 200 m of fluvio-deltaic sediments with well-bedded, grey, calcareous siltstones, greywackes and shales of the Fafanlap Formation which is of late Cretaceous age; the upper part of this formation contains 50 m of thinly bedded, partly nodular limestones. During the Cenozoic shallow marine sediments were laid down; these had a total thickness of only 300 m.

The Mesozoic sedimentary record of Misool shows very few affinities with the surrounding areas. In the Vogelkop (Bird's Head) there are no deposits of Jurassic age (FROIDEVEAUX, 1974). The Mesozoic record of Seram reveals discontinuous sequences of deep water deposits in the late Triassic to Miocene time interval (TJOKROSAPOETRO & BUDHITRISNA, 1982).

The Miocene deposits of Misool resemble those of Irian Jaya. On Misool the main phase of folding occurred in late Oligocene time, which resulted in an anticlinorium with a general plunge towards the ESE, the main axis of the anticlinorium being along the south coast of the island. In the southeast the inclined folds have steep north flanks that dip up to 60°. The intensity of folding rapidly decreases northward.

Within the structural framework of northeast

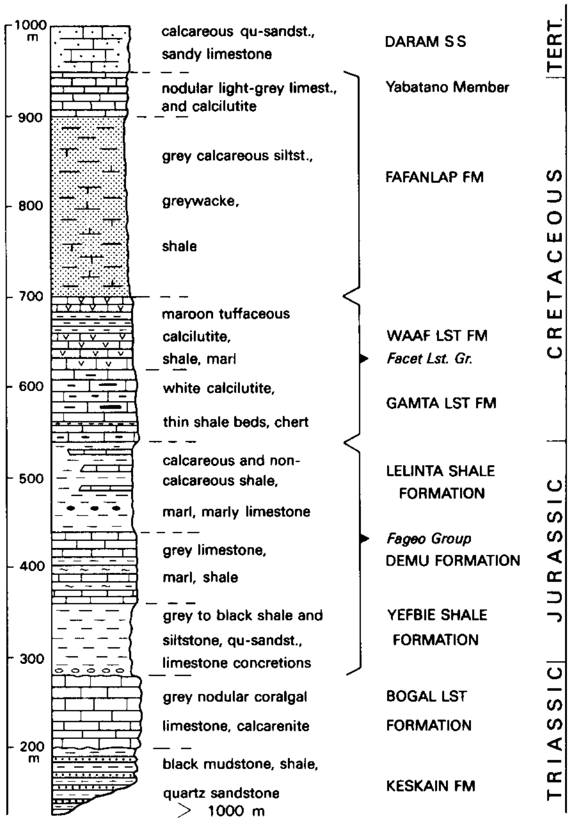

Fig. 2. Stratigraphic record of the Mesozoic of Misool, mainly after PIGRAM *et al.* (1982).

Indonesia, Misool is positioned in a block bounded by two fundamental east-west left-lateral transcurrent faults (Fig. 1): the Sorong Fault in the north, and the Tarera Fault in the south; the latter may continue westwards into the Seram Trough. Between Misool and Seram one comes across the right-lateral Bintuni Fault (FROIDEVEAUX, 1974; not mentioned by HAMILTON, 1979).

In the opinion of PIGRAM *et al.* (1982) the sedimentary and structural history of Misool fits in with the development of rift-drift sequences as subsequently elaborated in detail by PIGRAM & PANGGABEAN (1984) for northern and western Australia. The folding and subsequent faulting of the Triassic Keskain Formation, the deposition of the shallow marine Bogal Reef Limestones, and the post Bogal unconformity mark the period of 'break-up' with uplift and blockfaulting. The rifting in this area occurred somewhat earlier than in northwest Australia; this is in agreement with the supposition that rifting and subsequent drifting started in the northeast and gradually progressed towards the southwest along the west coast of the Australian continent. Consequently, the Island of Misool may form part of a microcontinent that drifted away from the main Australian continent in late Triassic-early Jurassic time.

3. PALAEOMAGNETIC PROCEDURES

3.1. SAMPLING IN THE FIELD

The palaeomagnetic sampling campaign on Misool was carried out along the south and southeast coasts and on a number of small islands south of the main island. In the field we used a portable drill provided with a coring tube of 25 mm inner diameter. Each sampled core was up to 10 cm long; in the laboratory the cores were cut into specimens, each having a length of 22 mm. A number of sites were selected at each sampling locality, usually in a particular rock formation. Between 6 and 10 cores were collected at each site.

Only sediments of Mesozoic age were sampled, because these rocks had been deposited mainly in deep water environments and bathyal sediments usually reveal stable remanences (J. van den Berg, pers. comm.).

Samples were collected (Fig. 1) from the Keskain Formation of middle Triassic age (MK); the Yefbie Shale Formation (MY), the Demu Limestone Formation (MD), and the Lelinta Formation (ML) which are of Jurassic age; and the Gamta Limestone Formation (MG), the Waaf Limestone Formation (MW), and the Fafanlap Formation (MF) which are of Cretaceous age. We sampled the Waaf Formation at four localities (Fig. 1). The sites MWA through MWE are located on the mainland between the Biga and Gam rivers; here, there are exposures of well-bedded, light grey calcilutites as well as greyish white to slightly brownish limestones with intercalations of shale. On the west coast of the Island of Kafal one comes across the sites MWF through MWI; the remaining sites are located on small islands to the north of the Waaf Islands: sites MWJ through MWM on Taptoponlek Island, and the sites MWN and MWO on Nubatpale Island. The Waaf Formation on these islands shows a corresponding lithology with well-bedded, maroon limestones in layers of 15 to 30 cm thickness alternating with grey marls, siltstones, or shales. The limestones are tuffaceous calcilutites.

The Fafanlap Formation was sampled at two localities to the northwest of the village of Fafanlap, one on each side of a large bay near Tangung Itaket (Cape Itaket): sites MFA and MFB on the right bank of the inlet, and sites MFC through MFG on the cape on the left bank. There are outcrops of medium-bedded to massive siltstones, well-bedded grey siltstones in layers 10 to 40 cm thick, and silty mudstones with some intercalated fine-grained sandstones and greywackes.

3.2. DETECTION OF THE CHARACTERISTIC REMANENCES

Unfortunately, at the laboratory it soon became apparent, that a large part of the collected material had very low intensities of natural remanent magnetization (NRM). These rocks cannot yield useful palaeomagnetic data, because, when the rocks were subjected to the partial demagnetization procedures, the sensitive magnetometers could no longer present reliable data. We were unable to obtain any consistent remanence directions from the specimens from two formations with fairly high initial NRM intensities, namely the Keskain Formation (MK) and the Yefbie Formation (MY) (Table 1).

In this paper palaeomagnetic data for two formations will be presented: the Waaf Formation of Santonian age (G. Thrupp, pers. comm.) and the Fafanlap Formation of early to middle Maastrichtian age (W.V. Sliter, pers. comm.*).

The specimens were treated with standard palaeomagnetic demagnetization procedures to determine both the intensity and the direction of the characteristic remanence. However, the initial remanence intensities of specimens from the Waaf sites MWA through MWE are very low with values between 0.008 and 0.020 $mA \cdot m^{-1}$ (Table 1). This is only slightly above the sensitivity of our magnetometer (0.002 $mA \cdot m^{-1}$). Therefore, these specimens are not included in further analysis.

The NRM of the remaining specimens, *i.e.* 121 from the Waaf Formation and 90 from the Fafanlap Formation, have been analysed either with alternating magnetic field (*af* method) or thermal progressive demagnetization. With some specimens the *af* method was not effective; these specimens subsequently were demagnetized further by heating. After each demagnetization step the specimens were measured on a 2G Enterprises cryogenic magnetometer.

Specimens analysed with alternating magnetic fields were treated in 7 successive steps up to a maximum peak value of 50 mT. The majority of the specimens, however, were treated with progressive thermal demagnetization: specimens from the Waaf Formation in 10 successive steps up to a maximum temperature of 630°C; specimens from the Fafanlap Formation in 9 to 12 successive steps up to maximum temperatures between 565°C and 640°C.

For the visual analysis of the results we used vector diagrams with orthogonal projections (ZIJDERVELD, 1967). The diagrams show that the initial remanence direction is usually built up of more than one component. Some examples are given in Fig. 3. Specimens MWK 1 and MFF 1 were treated with progressive heating. Both specimens show the presence of three components of remanence. Specimen MWK 1 has: 1. a viscous component that disappears after heating at 105°C; 2. a secondary component that is removed after heating at 500°C; 3. a component with high blocking temperature, because at subsequent progressive heating up to 600°C the direction of remanence does not change any more, and the magnetization vector decreases towards the origin of the projection. Specimen MFF 1 also reveals three components with abrupt changes in remanent direction after heating at 255°C and at 540°C. Specimens MWH 31 and MFF 51 were treated with alternating field only; they reveal three components of remanence as well with significant changes in direction after the application of *af* with peak values of 10 mT and of 32.5 mT.

Analysis with progressive *af* is not always successful for the detection of the characteristic remanence direction. We treated specimens MWO 11 and MFG 12 with *af* up to peak fields of 50 mT and subsequently we heated these specimens up to 600°C (Fig. 3). Both specimens reveal three components of remanence. Specimen MWO 11 has 1. a viscous component that is removed after *af* treatment with a peak value of 15 mT; 2. a secondary component that disappears after heating at 300°C; 3. a component with a high blocking temperature. Specimen MFG 12 very clearly shows changes in remanence direction after treatment with *af* at 25 mT peak value, and after heating at 350°C.

After careful application of the progressive demagnetization procedures the majority of the specimens from the Waaf and the Fafanlap Formations revealed characteristic remanence directions.

TABLE 1

Initial intensities of the natural remanent magnetization (NRM) of rocks collected on Misool. ($mA \cdot m^{-1}$ is milli-Ampere per metre.)

Formation	*Sites*	*NRM Intensity ($mA \cdot m^{-1}$)*
Keskain	MK	0.10 - 0.38
Yefbie	MY	0.05 - 0.80
Demu	MD	0.04 - 0.15
Lelinta	ML	0.008 - 0.130
Gamta	MG	0.008 - 0.020
Waaf	MWA - MWE	0.008 - 0.020
Waaf	MWF - MWO	1.5 - 60
Fafanlap	MF	3 - 12

**A joint paper will be prepared together with G. Thrupp, who also collected material on Misool for palaeomagnetic research, and with W.V. Sliter, who studied the microfossil content of some Mesozoic formations.*

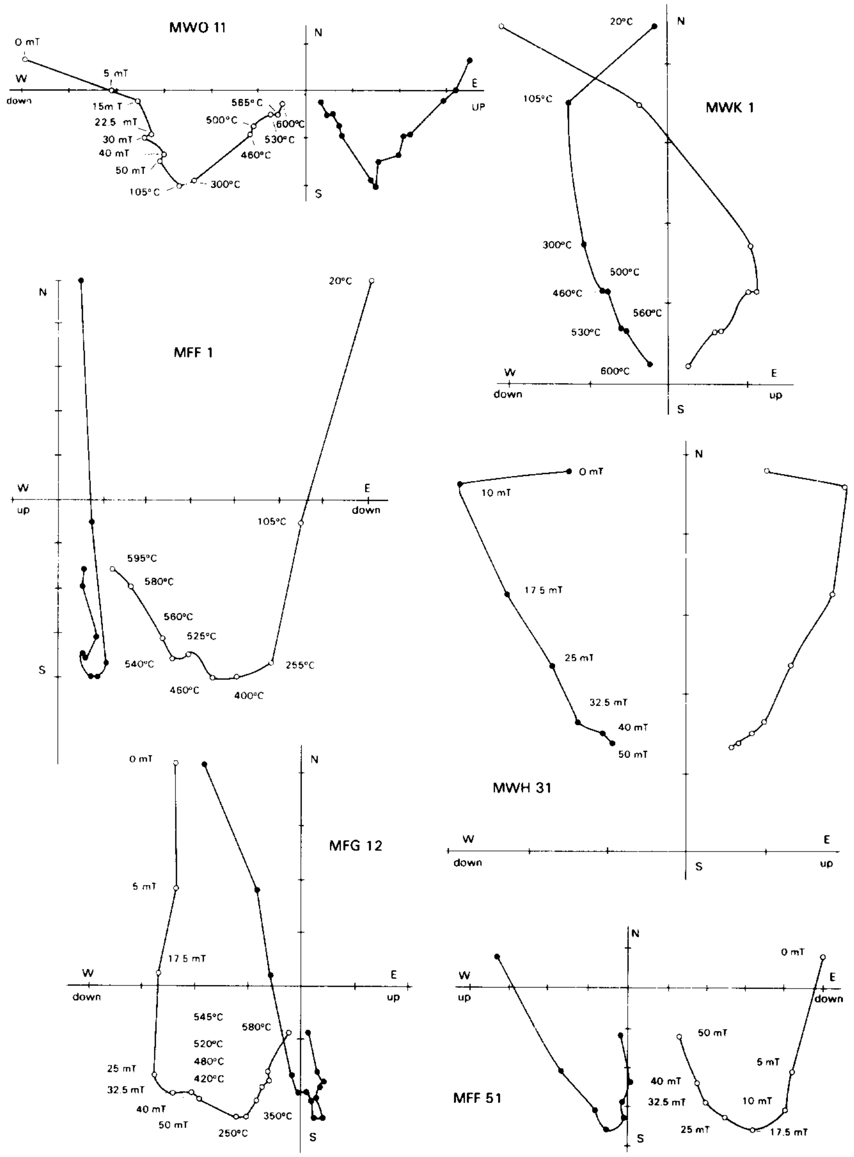

Fig. 3. Diagrams showing the progressive demagnetization of specimens from the Waaf (MW-) and the Fafanlap (MF-) Formations. The plotted points represent successive positions in orthogonal projection of the end of the resultant remanence vector during progressive demagnetization. Solid and open circles denote the projections on a horizontal and a vertical plane, respectively. Specimens MWK 1 and MFF 1 were thermally treated; specimens MWH 31 and MFF 51 were treated with alternating magnetic field (*af*); specimens MFG 12 and MWO 11 were demagnetized with *af* and, subsequently, by heating. In the diagrams each unit on either axis represents $2 \cdot 10^{-3}$ $A \cdot m^{-1}$ (specimens MWH 31, MFF 51, and MFG 12); $1 \cdot 10^{-3} A \cdot m^{-1}$ (specimen MFF 1); and $0.5 \cdot 10^{-3}$ $A \cdot m^{-1}$ (specimens MWO 11 and MWK 1).

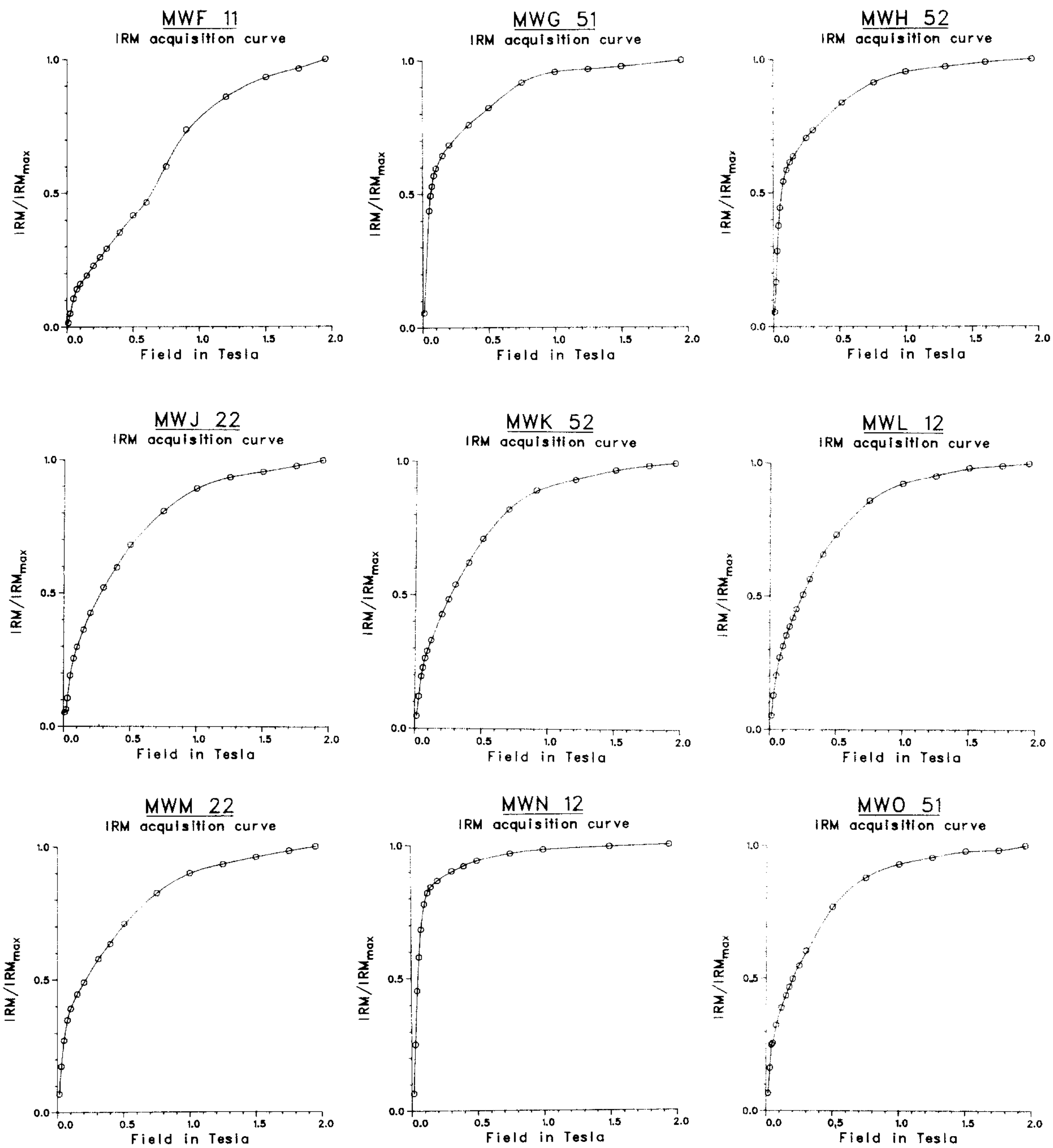

Fig. 4. Acquisition curves of Isothermal Remanent Magnetization of specimens from sites of the Waaf Formation, indicating the presence of both a low coercivity mineral (magnetite) and a high coercivity mineral (hematite and/or goethite).

3.3. ISOTHERMAL REMANENT MAGNETIZATION AND REMANENT COERCIVE FORCE

Normalized acquisition curves for the Isothermal Remanent Magnetization in direct fields up to 2 Tesla (IRM_{2T}) as well as the Remanence Coercive Force (H_{cr}) for the IRM_{2T} have been determined for one representative specimen of each site. These data may give us additional information concerning the carriers of remanence in our specimens. The IRM acquisition curves of specimens of sites from the Waaf Fm do not show identical patterns (Fig. 4). Specimens MWG 51, MWH 52, and MWN 12 show a rapid increase in IRM; after application of a direct field of only 300 mT they already had up to 70% to 90% of their maximum IRM. The shape of the curves is illustrative for the presence of a large proportion of magnetite as a carrier of remanence. The presence of fine-grained magnetite is supported by the fairly low values for H_{cr}: *e.g.* between 40 and 51.5 mT; in addition, the values for IRM_{2T}, ranging between 7.5 and 20.2 $A{\cdot}m^{-1}$, are rather high (Table 2). The presence of minerals of low coercivity, such as magnetite, can also be seen in the demagnetization diagrams. In specimen MWH 31 *af* treatment was successful for the detection of the ChRM component

TABLE 2

Remanent coercive force (H_{cr}) and isothermal remanent magnetization, after direct field of 2 Tesla (IRM_{2T}), of specimens from the Waaf and the Fafanlap formations. (Mt is milliTesla; $A{\cdot}m^{-1}$ is ampere per metre.)

Specimen	H_{cr} *(mT)*	IRM_{2T} *($A{\cdot}m^{-1}$)*	*Specimen*	H_{cr} *(mT)*	IRM_{2T} *($A{\cdot}m^{-1}$)*
MWF 11	295	2.35	MFA 72	37.5	4.19
MWG 51	51	7.49	MFB 72	41	3.62
MWH 52	51.5	9.52	MFC 42	39.2	5.27
MWI 22	162	1.21	MFD 22	40.5	9.35
MWJ 22	220	1.69	MFE 22	45	4.02
MWK 52	255	3.44	MFF 12	40	5.32
MWL 12	233	3.98	MFG 21	41.3	8.54
MWM 22	191	2.85			
MWN 12	40	20.17			
MWO 51	183.5	4.06			

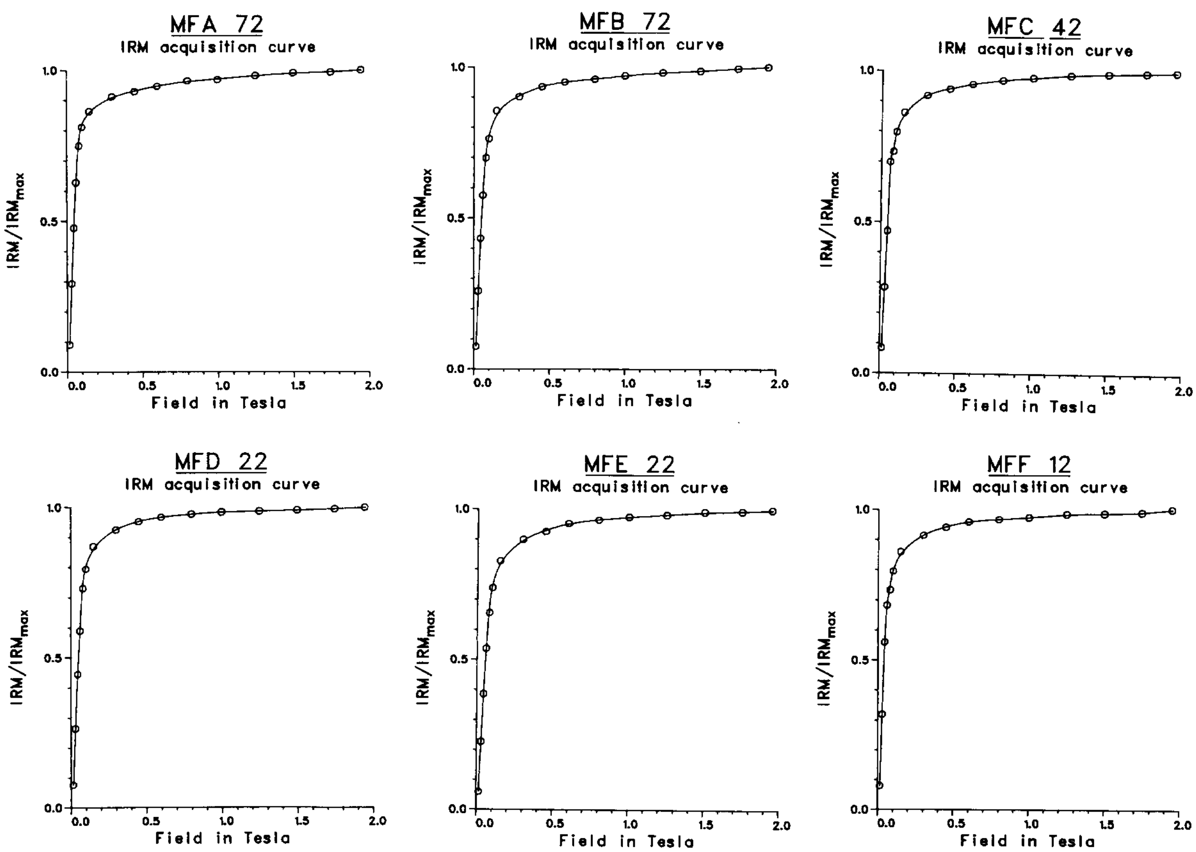

Fig. 5. Acquisition curves of Isothermal Remanent Magnetization of specimens from sites of the Fafanlap Formation, indicating the prevalent presence of a low coercivity mineral (magnetite).

TABLE 3

Palaeomagnetic data for the Waaf limestones of Misool, late Cretaceous (Santonian) age. Attitude is the strike and dip of the strata; N and E are the numbers of specimens included in, and excluded from the final analysis; af, Th, af+Th are treatments with alternating magnetic fields, heating, and alternating fields and subsequent heating, respectively; D and I are the declination and inclination in degrees of the characteristic NRM direction after bedding tilt correction; k is the precision parameter; a_{95} is the semi-angle of the cone of confidence, in degrees (FISHER, 1953).

Site	*Attitude*	*N*	*E*	*af*	*Th*	*af + Th*	*D*	*I*	*k*	a_{95}
MWF	84-37	13	0	1	11	1	320.4	−27.7	212	2.9
MWG	84-37	12	0	3	9	0	320.1	−28.2	257	2.7
MWH	84-37	12	0	2	10	0	319.7	−25.9	256	2.7
MWI	81-36.5	12	0	0	10	2	317.2	−33.2	176	3.3
MWJ	87-51	13	1	2	11	1	316.8	−44.7	48	6.0
MWK	82-52	11	1	1	9	2	316.0	−33.9	63	5.8
MWL	80-60	10	2	0	10	2	299.6	−28.6	113	4.6
MWM	83-60	13	0	2	11	0	318.2	−37.2	65	5.2
MWN	89-45	12	0	3	9	0	318.0	−36.2	206	3.0
MWO	89-45	13	0	0	11	2	129.9	41.0	27	8.2

after application of a field of 50 mT peak value; this is indicative of the presence of carriers of remanence of low coercivity. Thermal demagnetization of specimens from sites MWG, MWH, and MWN, however, shows that hematite may also be present as a carrier of remanence. The IRM acquisition curves for the specimens from the other Waaf sites (Fig. 4) show a slower increase of the IRM intensity with increasing direct field. After treatment in a direct field of 2 Tesla these specimens are not saturated. These patterns are indicative of the presence of a high coercivity mineral such as hematite or goethite. The specimens of these sites have rather high H_{cr} values and relatively low IRM_{2T} values (Table 2). The demagnetization diagrams for the specimens from these Waaf sites show that there is a viscous component of low intensity and a component with a high blocking temperature, *e.g.* hematite.

The normalized acquisition curve for specimen MWF 11 (Fig. 4) shows a linear increase between 100 mT and 600 mT, and steepens between 600 mT and 1 Tesla; this may point to the presence of goethite (LOWRIE & HELLER, 1982). However, the demagnetization diagrams for specimens from site MWF show that the viscous component has a rather low remanence intensity; thus, if goethite is present, it is probably not a carrier of remanence.

The normalized IRM acquisition curves for specimens from sites of the Fafanlap Fm have consistent shapes (Fig. 5). After application of a direct field of 300 mT the specimens have an IRM intensity of 90% of their maximum value. This is indicative of the presence of a mineral of low coercivity, *e.g.* magnetite (HARTSTRA, 1982; DUNLOP, 1986). When direct fields of a higher intensity have been applied the IRM curves show a slow, linear increase, which indicates the presence of a high coercivity mineral as well. The demagnetization diagrams for progressively heated Fafanlap specimens point to the presence of a high blocking temperature component, *i.e.* hematite. The H_{cr} data of the Fafanlap specimens (Table 2), illustrative for magnetite, indicate that if both hematite and magnetite occur as carriers of remanence, the latter is present in a much larger proportion.

4. PALAEOMAGNETIC RESULTS

The site-mean characteristic remanence direction (ChRM) with its statistical parameters has been computed from the data for individual specimens from each site. The palaeomagnetic results derived for the Waaf Limestones and those for the Fafanlap Siltstones are presented in Tables 3 and 4, respec-

TABLE 4

Palaeomagnetic data for the Fafanlap formation of Misool, late Cretaceous (Maastrichtian) age. For explanation of symbols see Table 3.

Site	*Attitude*	*N*	*E*	*af*	*Th*	*af + Th*	*D*	*I*	*k*	a_{95}
MFA	305-10	15	2	2	13	2	173.2	40.3	48	5.6
MFB	305-10	15	1	3	13	0	169.8	36.2	21	8.9
MFC	324-6	13	0	2	9	2	178.1	31.9	94	4.3
MFD	296-7	16	0	2	13	1	166.4	29.5	71	4.4
MFE	340-10	5	6	1	7	3	179.2	42.1	53	10.6
MFF	295-15	13	0	2	10	1	174.4	43.5	137	3.6
MFG	280-15	13	0	3	10	0	175.1	43.8	185	3.1

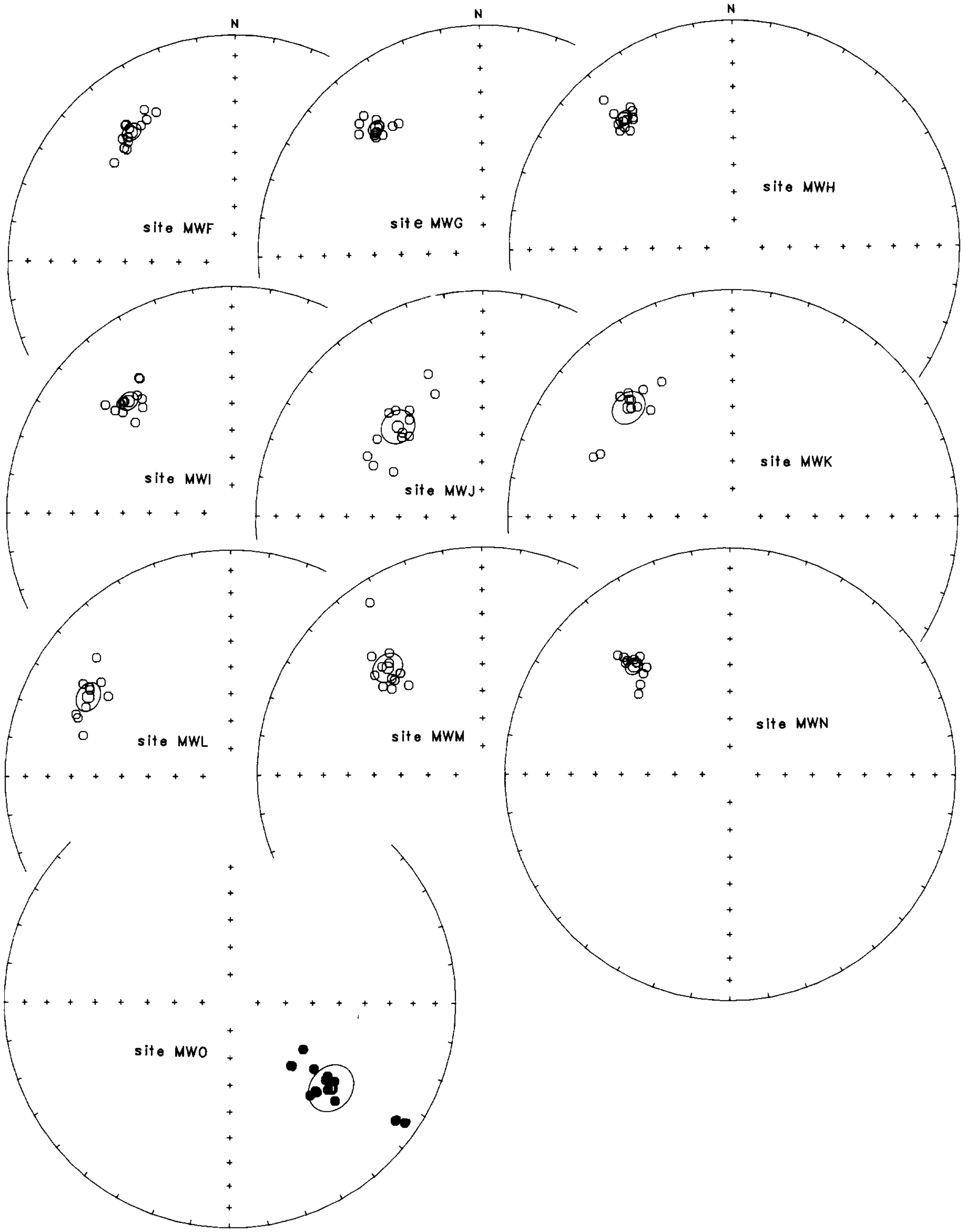

Fig. 6. Stereoplots of the Characteristic Remanence (ChRM) directions of specimens from sites of the Waaf Formation with the site mean directions provided with the circles of 95% confidence. Open and closed symbols denote upward-pointing directions and downward-pointing directions, respectively.

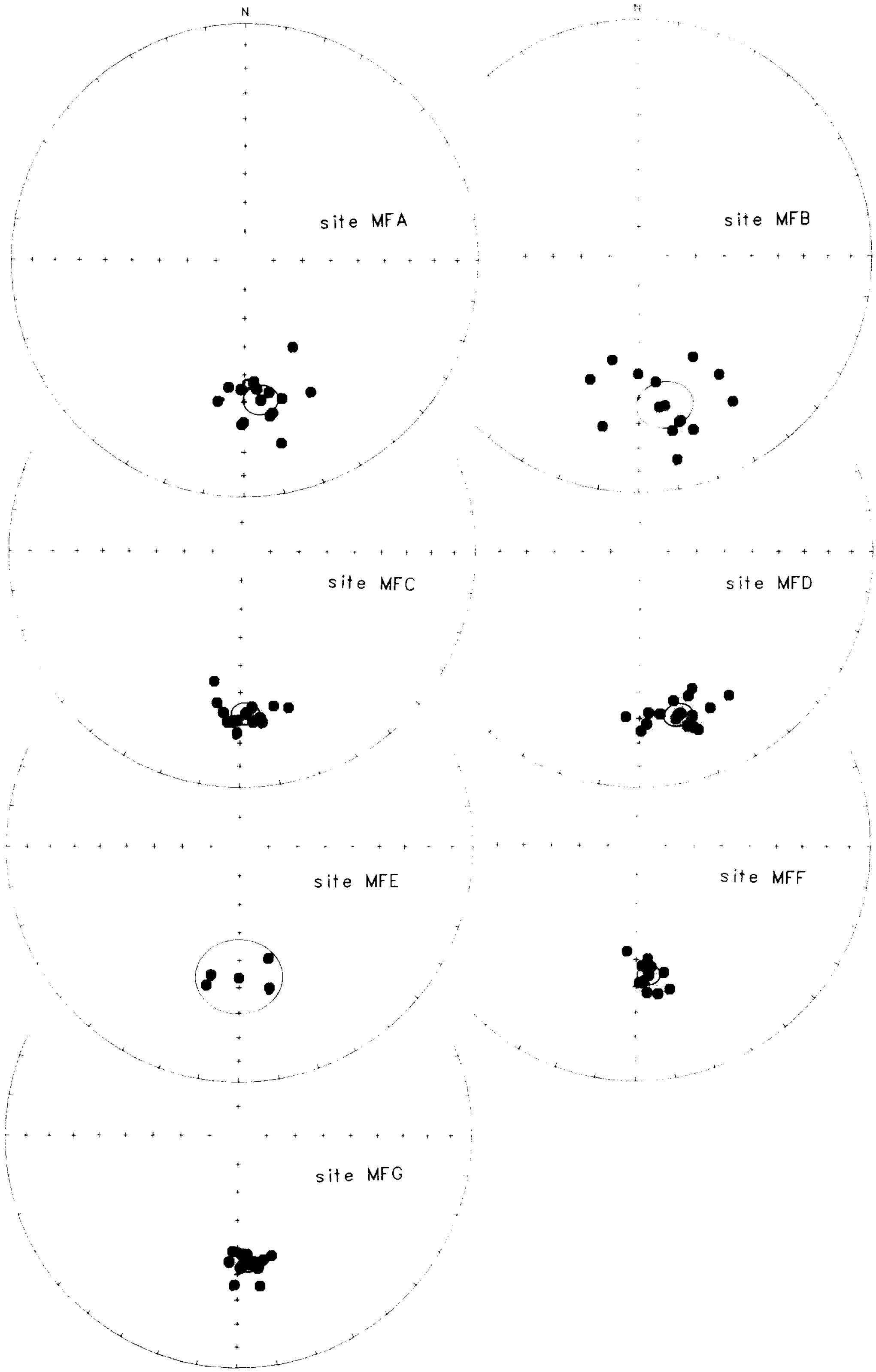

Fig. 7. Stereoplots of the ChRM directions of specimens from sites of the Fafanlap Formation with the site mean directions. See also caption Fig. 6.

TABLE 5

Mean characteristic remanence directions from Misool rock units of Cretaceous age, before tectonic correction. N is the number of sites included in the final analysis. For further explanation of symbols see Table 3.

Rock Unit	*Age*	*N*	*D*	*I*	*k*	a_{95}
Fafanlap Formation	Maastrichtian	7	177.8	30.3	153	4.9
Waaf Formation	Santonian	10	269.9	−58.0	37	8.1

tively. These tables list for each site, the attitude of the strata, and the number of specimens with the method of demagnetization applied.

The mean ChRM directions of both formations after tectonic correction are listed in Table 6, together with the between-sites statistical parameters. Stereoplots for the individual sites with the ChRM directions of their specimens, each provided with its site-mean direction and 95% confidence circle, are shown in Fig. 6 for the Waaf Fm and in Fig. 7 for the Fafanlap Fm.

The mean ChRM directions for all sites of these formations are plotted in the stereograms of Fig. 8. In this figure the lower projection of the Waaf Limestones shows the ChRM directions before tectonic correction. The Waaf Limestones reveal a positive fold test, because the value of a_{95} decreases from 8.1° before tectonic correction (Table 5) to 4.9° after tectonic correction (Table 6). Therefore, the characteristic remanence has a pre-main-folding age, *i.e.* pre-late Oligocene. There are arguments in favour of a syn- sedimentary or an early post-sedimentary origin for the remanence of the Waaf Limestones, because one out of ten sites—site MWO—revealed a ChRM with an opposite direction. The site-mean direction of the Waaf sites differs considerably from that of the present axial dipole field (Fig. 8). The fold-test applied to the Fafanlap Fm yields no significant result; the various sites of this formation have slight differences in attitude only. There are no reversals, but the site-mean ChRM direction of the Fafanlap sites differs considerably from the direction of the present field.

In Table 7 we have listed the palaeomagnetic pole positions of the Waaf and Fafanlap Fms which have been computed from the mean ChRM directions of these formations.

5. DISCUSSION OF THE RESULTS

In order to understand the Cretaceous palaeomagnetic results for Misool in a more extensive regional pattern, we shall compare them with data derived from nearby Australian rocks. The Australian polar wander curve for the time interval Carboniferous-early Tertiary shows a rather complicated course, and some parts of it are even incomplete. Three successive tracks can be

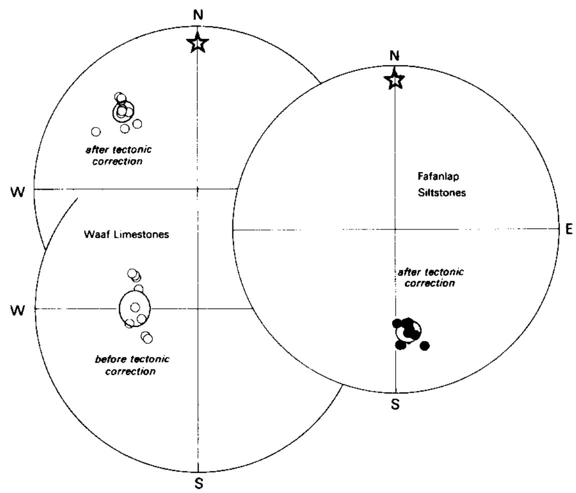

Fig. 8. Stereoplots with the site mean directions from the Waaf Limestones and the Fafanlap Siltstones with their overall mean provided with the circles of 95% confidence. For the Waaf Limestones the directions also are given before tectonic correction. The star marks the local direction of the present axial geocentric dipole field. See also caption for Fig. 6.

TABLE 6

Mean characteristic remanence directions from Misool rock units of Cretaceous age, after tectonic correction. N is the number of sites included in the final analysis. For further explanation see Table 3. Declination correction of 2.5°E applied.

Rock Unit	*Age*	*N*	*D*	*I*	*k*	a_{95}
Fafanlap Formation	Maastrichtian	7	176.1	38.3	143	5.1
Waaf Formation	Santonian	10	318.1	−33.8	97	4.9

TABLE 7
Palaeomagnetic pole positions from Misool rock units of cretaceous age. dp and dm are the semi-axes of the oval of 95% confidence for the pole position.

Rock Unit	*Age*	*Pole Position*				*Palaeolatitude*
		(°S)	*(°E)*	*dp*	*dm*	
Fafanlap Formation	Maastrichtian	69.7	140.8	3.6	6.0	21.5°
Waaf Formation	Santonian	45.8	195.5	3.2	5.6	18.5°

distinguished: a. between Carboniferous and Triassic a shift towards the east; b. in Jurassic time a westwards shift; and c. since the Middle Cretaceous a southerly trend (Fig. 9; Table 8). There are few Australian palaeomagnetic data for the time interval middle to late Jurassic through early Cretaceous, or for the late Cretaceous.

Thus, it is rather difficult to make an exact comparison between the pole positions derived from the Waaf and the Fafanlap Fms and those of Australian rocks of the same age.

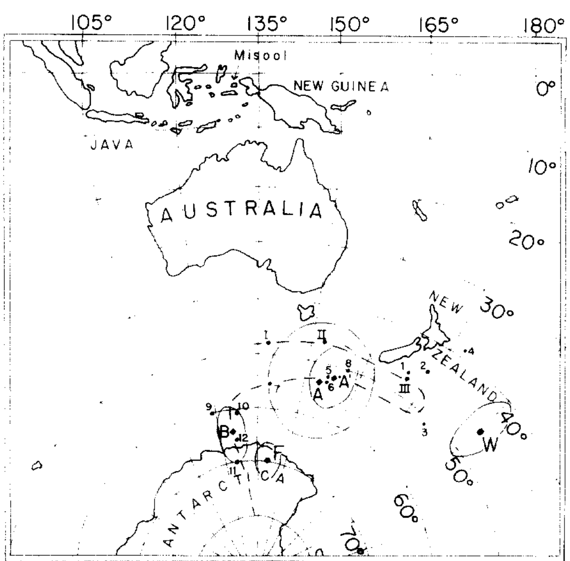

Fig. 9. Map of a part of the southern hemisphere between Indonesia and Antarctica showing the Australian Polar Curve since Carboniferous-Permian times. The pole positions identified by Latin and Arabic symbols are listed in Table 7. Poles A, A', and B are the mean Australian pole positions for the late Mesozoic (see also Table 7). The palaeomagnetic pole positions derived from both the Waaf Formation (W) and the Fafanlap Formation (F) are given as well. The poles A, A', B, W, and F are provided with their ovals of 95% confidence.

Nevertheless, there are some well-documented palaeomagnetic data of Australian rocks of late Mesozoic and early Tertiary age which can be used for comparison. The Waaf sediments most probably have an age of approximately 85 Ma. In Fig. 9 a mean Australian pole for the time interval 98 to 90 Ma derived from 3 poles (Table 8: 6', 7', 8) is indicated by A; the position of pole A' with a considerably lower value for a_{95} represents the mean of the same three poles listed in Table 8 with the original data from ROBERTSON & HASTIE (1962) and ROBERTSON (1963) for the poles 6 and 7, respectively. The Australian A poles and the Waaf (W) pole have widely different positions. The arc distance between A and Waaf is 28°, between A' and Waaf is 25°*.

The Fafanlap sediments have an age of approximately 70 Ma. The mean palaeomagnetic pole position of Australian rocks for the time interval 60 to 50 Ma derived from 4 palaeomagnetic data (Table 8: 9, 10, 11, 12) is indicated by B (Fig. 9). There are no data for Australian poles with ages around 70 Ma; therefore, the pole position F will be compared with Australian pole B. The poles B and F have statistically different positions as well; the arc distance is 8.5°.

In conclusion we can say that with the sampling localities at their present position the pole positions derived from rocks of Misool do not coincide with those derived from Australian rocks of approximately the same age.

Thus, in late Cretaceous time the crustal fragment of Misool must have occupied a position, with respect to the main Australian continent, which was different from its position today. The distance between Misool and Australia must have been greater than it is now. This is corroborated by the palaeolatitudinal positions of Misool in late Cretaceous time (Fig. 10).

The ChRM directions derived from the Misool formations permit us to establish the palaeolatitudinal positions of the areas of deposition in late Cretaceous time, using the formula $tg_{\text{latitude}} = 1/2\ tg_{\text{inclination}}$ (Table 7). In late Cretaceous time the

**We have not used the data listed by IRVING & IRVING (1982), because they include a pole derived from rocks of 81 Ma from New Zealand.*

TABLE 8

Palaeomagnetic pole positions from Australian rocks of Carboniferous to Eocene age References: (1) SCHMIDT, 1976a; SCHMIDT & MCDOUGALL, 1977; (2) SCHMIDT, 1976b; (3) ROBERTSON & HASTIE, 1962; (4) ROBERTSON, 1963; (5) IDNURM & SENIOR, 1978; (6) WELLMAN *et al.*, 1969; (7) IRVING *et al.*, 1961; (8) EMBLETON, 1981; (9) EMBLETON & SCHMIDT, 1977. Poles: pole A is the mean of the poles 6′, 7′, and 8 (6′ and 7′ recalculated by SCHMIDT (1976a), giving unit weight for site VGP positions); pole A′ is the mean of poles 6, 7, and 8; pole B is the mean of poles 9, 10, 11, and 12.

Rock Unit	*Age in Ma*	*Pole Position*			*Pole no.*	*Ref.*
		(°S)	*(°E)*	*(° a_{95})*		
Combined Eocene Basalts	60-40	60.8	127.6	9.4	12	(8)
Best Estimate for 50 Ma	50	65.7	126.8	10.0	11	(7)
Barrington Volcanoes	52	70.5	125.6	5.3	10	(6)
Mornay Profile	K-T	60.0	119.0	4.0	9	(5)
Bunbury Basalt	90	49.0	161.0	4.0	8	(2)
Mt. Dromedary Igneous Complex	93	55.0	139.0	8.0	7′	(1)
id.	93	56.0	138.0	9.0	7	(4)
Cygnet Alkali Complex	98	53.0	156.0	11.0	6′	(1)
id.	98	50.0	158.0	10.0	6	(3)
Tasmanian Dolerites	167	52.0	156.3	6.6	5	(1)
Kangaroo Island Basalts	170	39.0	183.0	11.0	4	(2)
Intrusives of New South Wales	174	51.0	186.1	10.9	3	(1)
Western Victoria Basalts	190	47.0	178.0	18.0	2	(2)
Garrawilla & Nombi Volcanics	193	46.1	175.2	10.0	1	(1)

Time Span	*Pole Position*			*Pole no.*	*Ref.*
	(°S)	*(°E)*	*(° a_{95})*		
60 - 50 Ma BP	64.3	124.8	5.7	B	
98 - 90 Ma BP	52.0	157.5	6.5	A′	
98 - 90 Ma BP	53.0	152.4	11.2	A	
Triassic-Jurassic	47.0	176.3	8.8	III	(9)
Permo-Triassic	46.8	153.6	17.4	II	(9)
Permo-Carboniferous	48.1	137.6	7.8	I	(9)

Australian continent was still connected to Antarctica. The more southerly position of Australia at 80 Ma is illustrated on a palaeocontinental map in Fig. 10 (SMITH *et al.*, 1981). On this map the palaeolatitudinal positions of the areas of deposition of both the Waaf sediments and the Fafanlap sediments are given at latitudes of 18.5° and 21.5° south, respectively. It is possible that in the time interval between the deposition of the Waaf and the subsequent Fafanlap formations the distance between Australia and Misool slightly decreased, but this decrease is not statistically significant (Fig. 10). From the ChRM data for the Misool rocks one can derive a polar distance of 71.5° for the Waaf Fm and a polar distance of 68.0° for the Fafanlap Fm; these are the arc distances between the sampling localities and their respective virtual palaeomagnetic pole positions. We shall use these polar distances in combination with the Australian poles (Waaf and pole A; Fafanlap and pole B) in order to find possible original locations of the Misool deposits with respect to the **present** position of the Australian continent.

In the first model we assume that Misool was situated at its present longitude of 130° E, but to the north of its location of today. Starting from the posi-

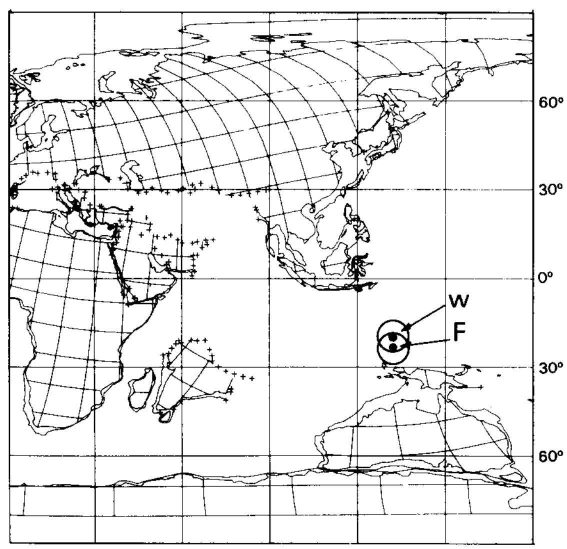

Fig. 10. Map showing the position of Australia 80 Ma ago according to SMITH *et al.* (1981) with the palaeolatitudinal position of Misool at an arbitrary longitude during the deposition of the Waaf (W) and the Fafanlap (F) sediments derived from palaeomagnetic research. The positions are provided with circles of 95% confidence.

tion of the Australian pole A, the polar distance of 71.5° (Waaf) results in a position at a latitude of 16° N for the Waaf sediments. According to the palaeomagnetic study of the Waaf sediments the position of Misool at a longitude of 130° E and a latitude of 16° N would result in a pole positioned at 52° S, 157.5° E (*i.e.* Australian pole A) if the ChRM declination had a direction of 337.4°. The present ChRM declination of the Waaf sediments is 318.1° (Table 6) and the present location of the deposits is at a latitude of 2° S. Therefore, it is possible that relative to the main Australian continent the sediments of the Waaf Fm shifted 18° to the south and performed an anticlockwise rotation of 19° (14° relative to pole A').

For a possible interpretation of the palaeomagnetic data from the Fafanlap Fm, we shall again assume that Misool was situated at its present longitude. With reference to the Australian pole B the polar distance of 68° deduced from the Fafanlap Fm would result in a latitude of 4° N and a ChRM declination of 186°. The present ChRM declination derived from the Fafanlap sediments is 176°. Thus, it is possible that since the deposition of the Fafanlap strata Misool has shifted 6° towards the south and performed an anticlockwise rotation of 10°.

If the original position of Misool was exactly to the north of its present position, this would mean that in the period between the deposition of the Waaf sediments and the subsequent Fafanlap sediments the island must have shifted 12° to the south and must have performed an anticlockwise rotation of 9°. Although these are large figures, on the palaeocontinental maps of Australia of 80 and of 60 Ma one can see that in this time interval the continent moved slightly to the south and also performed an anticlockwise rotation. After its break-away from Antarctica, approximately 53 Ma ago, the Australian continent moved rapidly towards the north. The distance between Misool and the main Australian continent could have been reduced to its present value during the folding phase in mid-Tertiary times in northeast Indonesia.

In the second model we assume that with respect to the Australian content Misool kept the same position in the time interval between the deposition of the Waaf and the subsequent Fafanlap sediments. If one again uses the Australian poles A and B, then, in this second model the position of the Island of Misool can be detected far to the west, at a longitude of 102° E and a latitude of 2° N. This would imply that since late Cretaceous time Misool has moved 28° towards the east and about 4° towards the south with an additional clockwise rotation of about 20°.

6. FINAL REMARKS

On the basis of our palaeomagnetic data both from Misool and from Australia we are not able to give exact positions for the Island of Misool relative to Australia for the late Cretaceous time interval. In this period the Australian palaeomagnetic information is rather poor. It is likely that Misool once formed part of the Australian continent, broke away in late Triassic-early Jurassic times, and moved away from Australia. The palaeomagnetic results derived from rocks of Misool indicate that in late Cretaceous time Misool had a position rather far to the north of Australia; its relative longitudinal position is not known. It is possible that in late Cretaceous time both Misool and Australia moved slightly to the south combined with an anticlockwise rotation. After the break-away from Antarctica about 53 Ma Australia moved rapidly to the north. The original distance between Misool and Australia could have been reduced during the late Oligocene folding phase in northeastern Indonesia. The late Cenozoic sense of movements along the transcurrent faults in northeastern Indonesia (Sorong Fault and Tarera Fault: Fig. 1) suggests that the block between these fundamental faults, which includes Misool, could have moved eastwards and could have rotated slightly clockwise. Therefore, it is concluded from the palaeomagnetic and geological data that we have available that Misool was originally located to the northwest or north-northwest of its present position relative to the Australian continent.

7. REFERENCES

BEMMELEN, R.W. VAN, 1949. The Geology of Indonesia. Martinus Nijhoff, The Hague: 1-732.

DUNLOP, D.J., 1986. Hysteresis properties of magnetite and their dependence on particle size: a test of pseudo-single domain remanence models.—J. geophys. Res. **91**: 9569-9584.

EMBLETON, B.J.J., 1981. A review of the Paleomagnetism of Australia and Antarctica. In: M.W. MCELHINNEY & D.A. VALENCIO. Paleoreconstructions of the continents. Geodyn. Ser. 2. A.G.U. Washington, D.C.: 77-92.

EMBLETON, B.J.J. & P.W. SCHMIDT, 1977. Revised paleomagnetic data for the Australian Mesozoic and a synthesis of late Paleozoic-Mesozoic results for Gondwana.—Tectonophysics **38**: 355-364.

FISHER, A.G., 1953. Dispersion on a sphere.—Proc. Royal Soc., London, Ser. A **217**: 295-305.

FROIDEVEAUX, C.M., 1974. Geology of Misool Island (Irian Jaya).—Proc. Indon. Petrol. Ass., 3rd. Ann. Convent.: 189-196.

HAMILTON, W., 1979. Tectonics of the Indonesian Region.—U.S. Geol. Surv. Prof. Paper 1078. U.S. Governm. Printing Off., Washington, D.C.: 1-345.

HARTSTRA, R.L., 1982. Grain-size dependence of initial susceptibility and saturation magnetization-related parameters of four natural magnetites in the PSD-MD range.—Geophys. J. R. astr. Soc. **71**: 477-495.

IDNURM, M. & B.R. SENIOR, 1978. Palaeomagnetic ages of Late Cretaceous and Tertiary weathered profiles in the Eromange Basin, Queensland.—Palaeogeogr., Palaeochim., Palaeoecol. **24**: 263-277.

IRVING, E., P.M. SCOTT & M.A. WARD, 1961. Demagnetization of igneous rocks by alternating magnetic fields.—Phil. Mag. **6**: 225-241.

IRVING, E. & G.A. IRVING, 1982. Apparent Polar Wander Path - Carboniferous through Cenozoic and the Assembly of Gondwana.—Geophysical Surveys **5**: 141-188.

LOWRIE, W. & F. HELLER, 1982. Magnetic properties of marine limestones.—Rev. Geophys. Space Phys. **20**: 171-192.

PIGRAM, C.J. & H. PANGGABEAN, 1984. Rifting of the northern margin of the Australian continent and the origin of some microcontinents in Eastern Indonesia.—Tectonophysics **107**: 331-353.

PIGRAM, C.J., H.B. CHALLINOR, F. HASIBUAN, E. RUSMANA & U. HARTONO, 1982. Geological results of the 1981 Expedition to the Misool Archipelago, Irian Jaya.—Bull. Geol. Res. Dev. Centre **6**: 18-29.

ROBERTSON, W.A., 1963. The Paleomagnetism of some Mesozoic Intrusives and Tuffs from Eastern Australia.—J. geophys. Res. **68**: 2299-2312.

ROBERTSON, W.A. & L. HASTIE, 1962. A paleomagnetic study of the Cygnet alkaline complex of Tasmania.—J. geol. Soc. Aust. **8**: 259-268.

ROGGEVEEN, P.M., 1939. Geologic Survey of North Misool.—B.P.M. Report, no. 1063.

SCHMIDT, P.W., 1976a. The non-uniqueness of the Australian Mesozoic palaeomagnetic pole position.—Geophys. J. R. astr. Soc. **47**: 285-300.

——, 1976b. A new paleomagnetic investigation of Mesozoic igneous rocks in Australia.—Tectonophysics **33**: 1-13.

SCHMIDT, P.W. & I. MCDOUGALL, 1977. Palaeomagnetic and potassium-argon dating studies of the Tasmanian Dolerites.—J. Geol. Soc. Austr. **25**: 321-328.

SMITH, A.G., A.M. HURLEY & J.C. BRIDEN, 1981. Phanerozoic palaeocontinental maps. Cambridge Earth Science Series, Cambridge Univ. Press, Cambridge: 1-102.

TJOKROSAPOETRO, S. & T. BUDHITRISNA, 1982. Geology of Seram.—Bull. Geol. Res. Dev. Centre **6**: 5-16.

WELLMAN, P., M.W. MCELHINNY & I. MCDOUGALL, 1969. On the polar wander path for Australia during the Cenozoic.—Geophys. J. **18**: 371-395.

ZIJDERVELD, J.D.A., 1967. A.C. demagnetization of rocks: analysis of results. In: D.W. COLLINSON, K.M. CREER & S.K. RUNCORN. Methods in Palaeomagnetism. Elsevier, Amsterdam: 254-286.